

Capacitance–voltage curve recovery of MOS capacitors passivated with BaF₂–BeF₂–SiO₂–B₂O₃–P₂O₅ glasses

Keiji Kobayashi

Toshiba ULSI Research Center, 1-Komukai Toshiba-cho Kawasaki, Japan

The capacitance–voltage (*C*–*V*) characteristics of metal-oxide–silicon (MOS) capacitors passivated by bubbled BaF₂–BeF₂–SiO₂–B₂O₃–P₂O₅ glasses with various water and fluoride contents have been investigated. As the absorption coefficients of OH[–] ions increased, adverse effects on the recovery of hysteresis loops of the *C*–*V* curves and their shifts were observed. The water content is related closely to the fluoride content in these glasses. A bubbling technique for blowing dry air through the molten glass during melting was effective for the removal of OH[–] ions in the fluoride-containing glasses.

Borophosphosilicate glass films formed by inorganic gas-phase chemical vapour deposition have been used widely in high-density integrated circuits as dielectric insulators.^{1–3} The advantageous properties of such films are conformable step coverage, effective protection against alkali-metal ions, and a fairly low softening temperature. Highly doped borophosphosilicate glasses flow at low temperatures to give rounding at the edge of glasses used for coating ultra-high-density integrated circuits, but they also suffer from a tendency to crystallize during this process.⁴ Such crystallization is a serious drawback in the lamination of ultra-high-density integrated circuits.⁴ Low-temperature glass flow has been studied and used to prepare planar MOS devices and to fabricate multi-level interconnections.^{5,6} It is thought that glass flow is controlled by viscosity, which in turn is controlled by composition, chemical bonding⁷ and structure.^{8,9} Thus, a glass with ‘low connectivity’⁷ and ‘a released structure’⁸ is less viscous than a glass without such characteristics. It is expected that fluoride-containing glasses with ionic bonds would have lower viscosities than related oxide glasses.

It has been found that zinc borosilicate glasses have lower softening temperatures than borophosphosilicate glasses, and do not suffer from the problem of crystallization during flow.^{5,6} Both borophosphosilicate and zinc borosilicate glasses contain small amounts of water,^{10,11} and this has an adverse effect on the *C*–*V* characteristics of MOS devices if they are heated rapidly. It is difficult to quantify the small amount of water in these glasses using the water absorption band in the transmission IR spectra and, therefore, we tried to use the absorption coefficient of OH[–] ions calculated from the IR spectra to evaluate these glasses. The shift of *C*–*V* curves in silicon devices is caused by the surface charges associated with polarizable ions.¹² Previous studies have shown that the abnormal *C*–*V* curves of MOS capacitors are a result of highly polarizable ions and OH[–] ions in the glass.^{11–13} Radicals do not carry a charge, but Li *et al.*¹³ demonstrated that OH[–] ions exercise an adverse influence over the hysteresis of MOS capacitors.

In this paper, we discuss the relationship between absorption of OH[–] ions and shifts in the *C*–*V* curve for MOS capacitors passivated using bubbled BaF₂–BeF₂–SiO₂–B₂O₃–P₂O₅ glasses containing small amounts of OH[–] ions, and investigate the application of these glasses to MOS capacitors.

Experimental

BaF₂–BeF₂–SiO₂–B₂O₃–P₂O₅ glasses were prepared from 1 kg batches of reagent-grade chemicals melted at 1400 °C for 5 h in an ultra-high-purity platinum crucible in an electric furnace in an oxidizing atmosphere. Dry air was blown through the liquid glass for 1 h during melting in an oxidizing atmosphere

using a platinum tube (the ‘dry-air-bubbling’ technique¹⁰). After melting, the glass was poured onto a stainless-steel plate and annealed.

Transmission IR spectra were measured using a Digi-Lab spectrophotometer with 10 × 20 × 1 mm³ plates. Glass-flow points *T_f* (log η = 5.0, where η is the viscosity) were obtained from thermal expansion curves, using a method described previously, where the flow point was defined.¹⁴

Sputter targets were cut from these samples and ground to a diameter of 75 mm and a thickness of 10 mm. Glass films 0.5 µm thick were deposited on an SiO₂ layer (0.3 µm) on Si(100) wafers under 1 kW power and 30 mTorr vacuum sputtering conditions using a Perkin-Elmer vacuum system. The glass thickness was measured by the use of a Nanometrics SD9-2000T thickness meter using the Na D line refractive index (n_D = 1.56, measured by a refractometer). Aluminium electrodes were deposited on the glass films. *C*–*V* curves for these MOS capacitors were observed at 1 MHz at room temperature, as described previously.¹⁵

Results and Discussion

The chemical compositions (mol%) of various glasses, their absorption coefficients, β_{OH} , flow points, *T_f*, and *C*–*V* curve shifts, ΔV_G , are listed in Tables 1 and 2. Transmission IR spectra for these glasses are given in Fig. 1 and 2. The absorption bands around 3500 cm^{–1} are due to fundamental vibrations arising from OH[–] ion absorption.^{16–18}

The relationship between transmittance, T_{OH} , and reflectivity, R_{OH} , can be represented as follows:¹⁸

$$T_{OH} = 1 - [R_{OH}(1 - R_{OH}) + R_{OH}] = (1 - R_{OH})^2 \quad (1)$$

The absorption coefficient, β_{OH} , resulting from the fundamental vibration due to OH[–] ions at around 3500 cm^{–1}, is calculated from eqn. (2).¹⁹

$$T_{OH} = [(1 - R_{OH})^2 \exp(-\beta_{OH}t)] / [1 - R_{OH}^2 \exp(-2\beta_{OH}t)] \quad (2)$$

where *t* is the glass thickness.

The absorption coefficient of OH[–] ions is a function of OH[–] or H₂O concentration. In this respect, all the glasses with various OH concentrations affect the electrical properties of MOS capacitors. Combination of eqn. (1) and (2) leads to

$$\exp(-\beta_{OH}t) + R_{OH}^2 \exp(-2\beta_{OH}t) = 1 \quad (3)$$

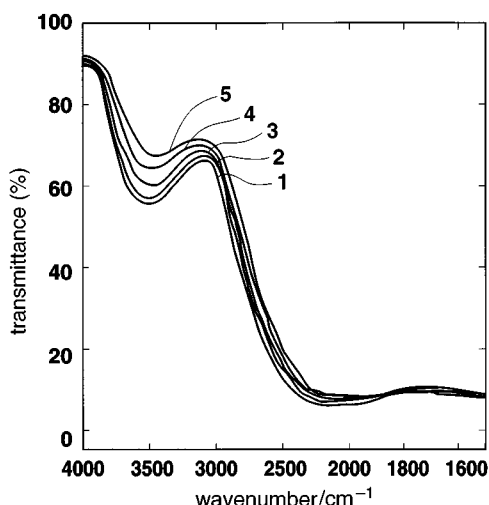
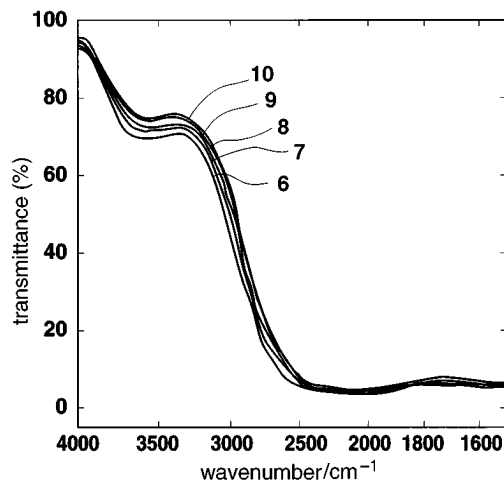
Values of β_{OH} for OH[–] ions are computed from eqn. (3). Values of T_{OH} , R_{OH} and β_{OH} calculated from the IR transmission spectra in Fig. 1 and 2 are also listed in Table 1 and 2. The

Table 1 Glass compositions, T_{OH} , R_{OH} , β_{OH} , T_f and ΔV_G (glasses 1–5 are without bubbling)

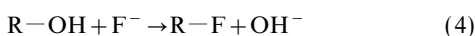
| glass | composition (mol%) | | | | | $T_{\text{OH}}\text{ (%)}$ | R_{OH} | $\beta_{\text{OH}}/\text{cm}^{-1}$ | $T_f/^\circ\text{C}$ | $\Delta V_G/\text{V}$ |
|-------|--------------------|----------------|----------------|------------------------|------------------------|----------------------------|-----------------|------------------------------------|----------------------|-----------------------|
| | BaF_2 | BeF_2 | SiO_2 | P_2O_5 | B_2O_3 | | | | | |
| 1 | 2 | 1 | 27 | 50 | 20 | 55 | 0.26 | 0.61 | 780 | 3.0 |
| 2 | 4 | 2 | 24 | 50 | 20 | 56 | 0.25 | 0.59 | 770 | 2.5 |
| 3 | 6 | 3 | 21 | 50 | 20 | 59 | 0.23 | 0.50 | 760 | 2.2 |
| 4 | 8 | 4 | 18 | 50 | 20 | 62 | 0.21 | 0.41 | 755 | 1.7 |
| 5 | 10 | 5 | 15 | 50 | 20 | 65 | 0.19 | 0.36 | 750 | 1.2 |

Table 2 T_{OH} , R_{OH} , β_{OH} , T_f and ΔV_G for glasses 6–10 (which correspond to glasses 1–5, respectively, which have been dry-air-bubbled)

| glass | $T_{\text{OH}}\text{ (%)}$ | R_{OH} | $\beta_{\text{OH}}/\text{cm}^{-1}$ | $T_f/^\circ\text{C}$ | $\Delta V_G/\text{V}$ |
|-------|----------------------------|-----------------|------------------------------------|----------------------|-----------------------|
| 6 | 68 | 0.17 | 0.35 | 781 | 1.4 |
| 7 | 70 | 0.16 | 0.23 | 771 | 1.3 |
| 8 | 72 | 0.15 | 0.20 | 758 | 1.1 |
| 9 | 74 | 0.14 | 0.18 | 754 | 0.8 |
| 10 | 76 | 0.13 | 0.15 | 749 | 0.6 |

**Fig. 1** Transmission IR spectra for $\text{BaF}_2\text{--BeF}_2\text{--SiO}_2\text{--B}_2\text{O}_3\text{--P}_2\text{O}_5$ glasses without bubbling**Fig. 2** Transmission IR spectra for dry-air-bubbled $\text{BaF}_2\text{--BeF}_2\text{--SiO}_2\text{--B}_2\text{O}_3\text{--P}_2\text{O}_5$ glasses

transmission IR spectra of these glasses show a decrease in the intensities of the absorption bands of OH^- ions with increasing fluoride content. A part of the fluorine is incorporated into the glass network and reacts with OH^- ions:



Fluoride compounds react with water in the batch during melting:



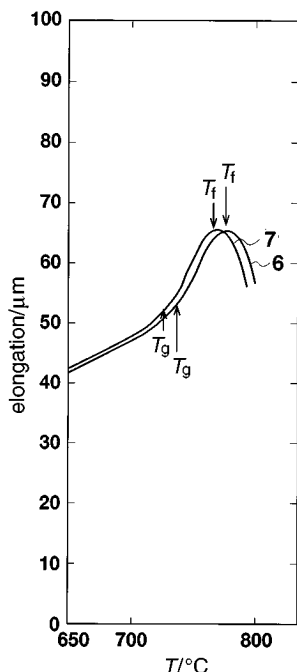
where $\text{R} = \text{Ba, Be}$.

Consequently, the reaction of water with fluoride groups in the glasses would be advantageous as a means of reducing the IR absorption bands due to water. Furthermore, the dry-air-bubbling technique is effective for the removal of OH^- ions in glasses, as shown by comparing Fig. 1 and 2. The glasses might contain water, even after bubbling with dry air, as the expulsion of water from the glasses is dependent on their composition.

Thermal expansion curves of $\text{BaF}_2\text{--BeF}_2\text{--SiO}_2\text{--B}_2\text{O}_3\text{--P}_2\text{O}_5$ glasses are given in Fig. 3 and 4, which also show the transition points (T_g) and the glass-flow points (T_f). With regard to the $C\text{--}V$ curve shifts in MOS capacitors, when the absorption coefficients of OH^- ions increase, ΔV_G shifts and hysteresis also increase.

The $C\text{--}V$ characteristics of MOS capacitors passivated with these glasses are shown in Fig. 5 and 6. All the $C\text{--}V$ curves for capacitors passivated with these glasses shift towards the right. Thus, these peculiar $C\text{--}V$ characteristics represent the recovery of $C\text{--}V$ curve shifts as the absorption coefficients of OH^- ions decrease.

The loss of hydrogen and hydroxy species is related to the disappearance of $C\text{--}V$ hysteresis. The hydrogen and hydroxy defects are responsible for the polarizing mechanism. This shift is related to hydrogen- and hydroxy-related vacancies in water-containing glasses.

**Fig. 3** Typical thermal expansion curves for dry-air-bubbled $\text{BaF}_2\text{--BeF}_2\text{--SiO}_2\text{--B}_2\text{O}_3\text{--P}_2\text{O}_5$ glasses 6 and 7

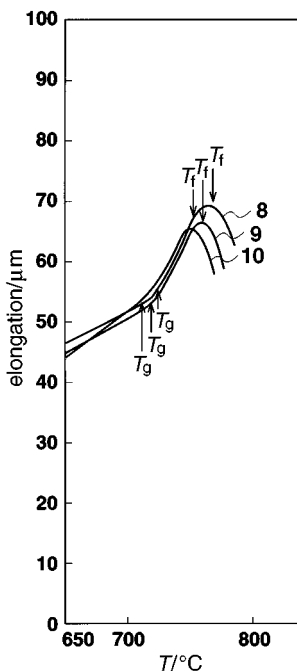


Fig. 4 Typical thermal expansion curves for dry-air-bubbled $\text{BaF}_2\text{-BeF}_2\text{-SiO}_2\text{-B}_2\text{O}_3\text{-P}_2\text{O}_5$ glasses

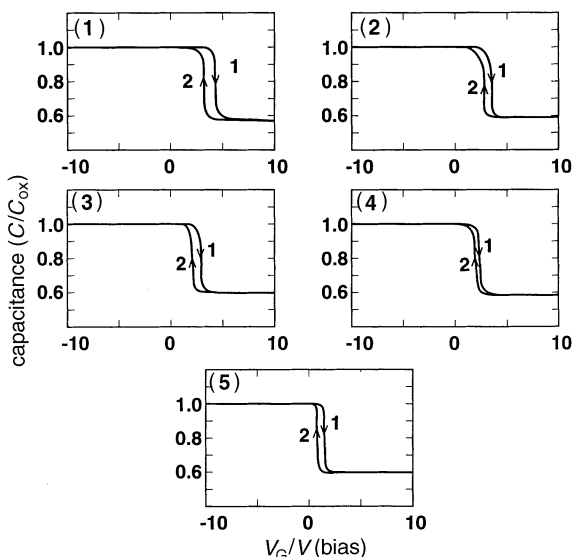


Fig. 5 $C\text{-}V$ curve characteristics of thermally annealed MOS capacitors passivated by $\text{BaF}_2\text{-BeF}_2\text{-SiO}_2\text{-B}_2\text{O}_3\text{-P}_2\text{O}_5$ glasses without bubbling. 1, forward curve; 2, reverse curve.

With increasing β_{OH} , the $C\text{-}V$ curves shift towards the right. The mean $C\text{-}V$ curve shifts, ΔV_g , at the midpoint of the forward and reverse hysteresis curves are summarized in Table 1 and 2.

The hysteresis curves for these MOS capacitors showed good reproducibility, as required for the passivation of MOS device.

Conclusions

A reduction in the viscous flow point of the glasses studied appears to correlate with an increase in fluoride content and a decrease in OH^- absorption coefficient. The OH^- absorption coefficient decrease may be due to the fluoride content of the molten glasses.

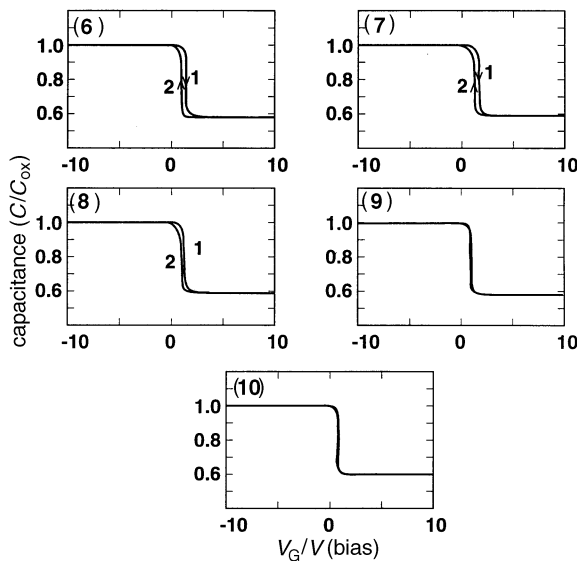


Fig. 6 $C\text{-}V$ curve characteristics of thermally annealed MOS capacitors passivated by dry-air-bubbled $\text{BaF}_2\text{-BeF}_2\text{-SiO}_2\text{-B}_2\text{O}_3\text{-P}_2\text{O}_5$ glasses

The MOS capacitors passivated with $\text{BaF}_2\text{-BeF}_2\text{-SiO}_2\text{-B}_2\text{O}_3\text{-P}_2\text{O}_5$ glasses containing low concentrations of water exhibited the best recovery of their $C\text{-}V$ characteristics. With increasing OH^- absorption coefficient, an adverse effect was seen on the recovery of hysteresis $C\text{-}V$ curve shifts. The dry-air-bubbling technique was effective for the removal of OH bands. Hysteresis and V_g shifts for MOS capacitors passivated with bubbled fluoride-containing glasses were improved; in particular, some MOS capacitors showed no hysteresis curve. After heating, the recovery of hysteresis and ΔV_g shifts for these MOS capacitors showed good reproducibility, as required for MOS device passivation. The relationship between recovery from the peculiar hysteresis $C\text{-}V$ curve shifts and OH^- absorption coefficient is discussed briefly.

The author would like to thank Dr. H. Sasaki in the Toshiba Research and Development Center for the measurement of transmission IR spectra.

References

- 1 K. H. Hurley, *Solid State Technol.*, 1987, **30**, 103.
- 2 J. E. Dickinson Jr. and B. H. W. S. deJong, *J. Non-Cryst. Solids*, 1988, **102**, 196.
- 3 N. F. Raley and D. L. Losee, *J. Electrochem. Soc.*, 1988, **135**, 2640.
- 4 G. L. Schnable, A. W. Fisher and J. M. Shaw, *J. Electrochem. Soc.*, 1990, **135**, 3973.
- 5 K. Kobayashi, *J. Non-Cryst. Solids*, 1986, **88**, 229.
- 6 K. Kobayashi, *J. Non-Cryst. Solids*, 1994, **176**, 208.
- 7 K. Kobayashi, *J. Non-Cryst. Solids*, 1993, **159**, 274.
- 8 K. Kobayashi, *Glass Technol.*, 1988, **29**, 253.
- 9 K. Kobayashi, *Glass Technol.*, 1989, **30**, 110.
- 10 K. Kobayashi, *J. Electrochem. Soc.*, 1984, **131**, 2190.
- 11 S. Rojas, R. Gomarasca, L. Zanotti, A. Borghesi, A. Sassel, G. Ottaviani, L. Moro and P. Lazzeri, *J. Vac. Sci. Technol. B*, 1992, **10**, 633.
- 12 K. Kobayashi, *J. Solid State Chem.*, 1995, **120**, 54.
- 13 S. C. Li, S. P. Murarka, X. S. Guo and W. A. Lanford, *J. Appl. Phys.*, 1992, **72**, 2947.
- 14 G. Baret, R. Madar and C. Bernar, *J. Electrochem. Soc.*, 1991, **138**, 2835.
- 15 K. Kobayashi, *J. Non-Cryst. Solids*, 1990, **124**, 229.
- 16 C. M. Shaw and J. E. Shelby, *Phys. Chem. Glasses*, 1993, **34**, 35.
- 17 K. Kobayashi, *Glass Technol.*, 1993, **34**, 120.
- 18 J. A. Ruller and J. E. Shelby, *Phys. Chem. Glasses*, 1992, **33**, 177.
- 19 Z-H. Liang and G. H. Frischat, *J. Non-Cryst. Solids*, 1993, **163**, 169.